Field Cases Analysis of Protection Schemes Applied to Transmission Lines Connecting Inverter-Based Resources to the Grid

Marcelo Bini
EDF Renewables

Ricardo Abboud, Fabio Lollo, and Paulo Lima
Schweitzer Engineering Laboratories, Inc.

Presented at the
27th Annual Georgia Tech Fault and Disturbance Conference
Atlanta, Georgia
April 13–14, 2026

Originally presented at the
52nd Annual Western Protective Relay Conference, October 2025

Field Cases Analysis of Protection Schemes Applied to Transmission Lines Connecting Inverter-Based Resources to the Grid

Marcelo Bini, *EDF Renewables*
Ricardo Abboud, Fabio Lollo, and Paulo Lima, *Schweitzer Engineering Laboratories, Inc.*

***Abstract*—In this paper, we present and discuss the protection scheme that EDF Renewables Brazil defined as the standard for their extra-high voltage transmission lines that connect renewable sources to the grid, including transient- and phasor-based elements. This paper includes our analysis of field events involving the standardized protection system, which has been in operation for over two years on the utility's 500 kV transmission lines. We also evaluate the performance of the applied protection functions for real faults, including both external and internal faults on the protected transmission lines. Our analysis of field-event reports demonstrates the benefits of the combined protection system.**

I. Introduction

The increasing penetration of renewable energy sources, such as wind farms and photovoltaic (PV) solar plants, introduces new challenges for protecting the transmission lines that connect these sources to the bulk power system. These challenges arise from the distinct fault-current contribution characteristics of renewable sources compared to traditional synchronous generators, leading to issues with protection-scheme speed, sensitivity, security, dependability, and selectivity.

Due to the unconventional nature of renewable sources, the security of phasor-based protection applications often relies on conservative, security-oriented settings. While this approach prevents unnecessary protection trips, it typically results in reduced sensitivity and slower response times than in traditional applications. In contrast, transient-based protection methods—such as those based on traveling waves and incremental quantities—respond to the dynamic changes in current and voltage caused by faults, making them independent of source type and more robust in renewable-rich environments.

The utility built and now operates several wind and solar plants across the country. Based on their extensive field experience, the utility has standardized their approach to protecting the connecting transmission lines using a protection scheme that combines phasor-based and transient-based elements and schemes for the transmission lines that connect their renewable plants to the grid. This innovative approach offers significant improvements in protection speed, security, and reliability. Furthermore, this approach uses traveling waves to locate faults with an accuracy of approximately one tower span.

In Section II, we present a brief review of the impact of nonconventional sources on transmission line protection, and in Section III, we introduce key transient-based protection principles. In Section IV, we describe and discuss the standardized protection scheme adopted by the utility for its extra-high voltage transmission lines. In Section V, we analyze real-world fault events involving this protection system, evaluating the performance of the applied protection functions during both internal and external faults. We demonstrate the benefits of protection schemes that use both phasor- and transient-based methods through a detailed analysis of field-event reports, followed by our conclusion.

II. Impact of IBRs on Transmission Line Protection

The behavior of unconventional power sources, such as IBRs and wind induction generators, during network faults differs from traditional synchronous generators (SGs). SGs are high-inertia machines and have the capacity to maintain their operational condition for multiple power cycles after fault inception. In the case of unconventional sources, a sudden variation in operational conditions may happen according to the control action. Furthermore, the IBR fault-current contribution is restricted by the capacity of its power electronic components and its control functions. Typically, the maximum current capacity of these power components does not exceed 1.5 times the rated current during the steady-state fault condition, due to design and economic factors [1].

The atypical behavior and characteristics of unconventional sources during system faults may challenge the reliability of the traditional phasor-based protection functions, because the physics considered in their design are no longer valid. Fig. 1 shows a line relay field-event record with the currents and voltages for a Phase-B-to-ground fault on the transmission network near a PV power plant. For this event, the relay was located at the PV side of the transmission line connecting the power plant to the grid. The atypical fault-current contribution from the IBR is illustrated starting at the 0 ms mark, with low magnitude and heavily distorted currents.

Due to low or no mechanical inertia, currents and voltages supplied by unconventional sources may have angle and frequency variations. In the case of an SG, the relationship between the negative-sequence current and negative-sequence voltage is determined by the generator negative-sequence impedance. However, in the case of an unconventional source, it follows that the control design, and the angle between the negative-sequence current and negative-sequence voltage, may vary indiscriminately during the fault, as the injected current

may not produce a proportional voltage according to the equivalent impedance of the source. In other words, the negative-sequence current and negative-sequence voltage are not governed by the laws of physics, and their behavior cannot be accurately simulated without a detailed control model, which is often unavailable.

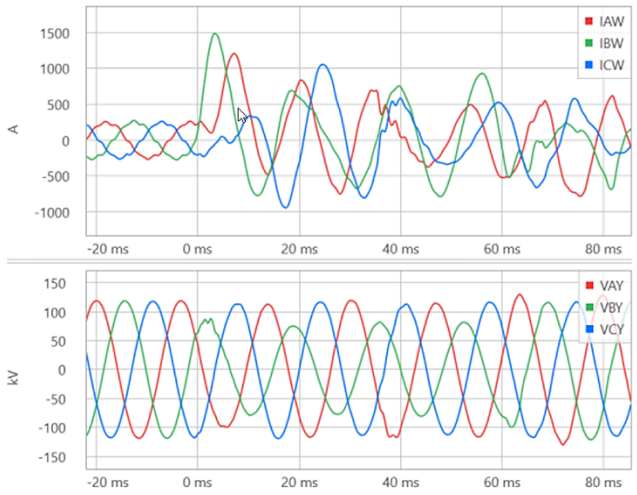

Fig. 1. Field-event record of currents and voltages at the PV plant point-of-connection for the B-G fault.

Fig. 2 shows a 420 MW PV power plant and the transmission line connecting it to the grid transmission network. To illustrate how the atypical fault contribution from an IBR challenges traditional protection, we evaluate the performance of line protection—including fault-type identification, negative-sequence directional, mho distance, and current differential—for an external Phase-A-to-ground (AG) field fault. Fig. 3 plots phase currents and voltages recorded by the relays at the PV line terminal for this field event.

Some implementations of fault-type identification logic compare the angle between the negative-sequence current and zero-sequence current phasors to determine the faulted phase(s) [2]. In the case under analysis, the angle of the negative-sequence current phasor changes in relation to the angle of the zero-sequence current phasor. Consequently, the fault-type identification logic misidentifies the faulted phase, as illustrated by the activation of FSA, FSB, and FSC in Fig. 4.

Fig. 2. Simplified one-line diagram of the PV plant connection to the grid transmission network.

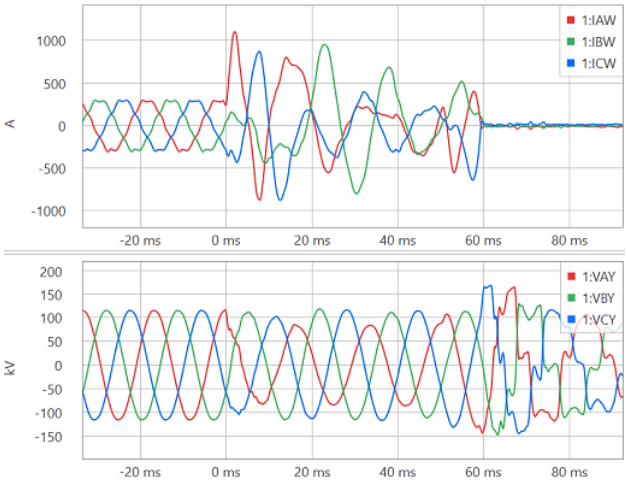

Fig. 3. Raw event record with line currents and voltages at PV plant point-of-connection for the external AG fault.

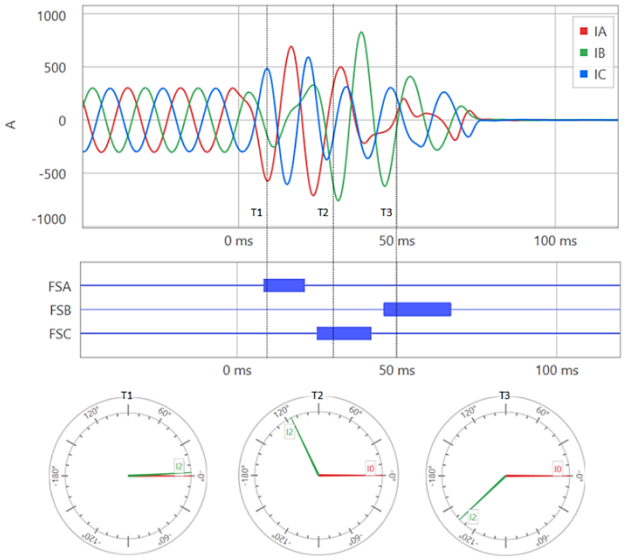

Fig. 4. Fault current and behavior of I_2 in relation to I_0 during AG fault in different fault moments.

In the negative-sequence directional element, the angle between the negative-sequence voltage phasor (V2) and the negative-sequence current phasor (I2) determines the fault direction. For a forward fault, the negative-sequence current shifted by the line angle (I2R) is expected to be 180 degrees out of phase with V2; however, for a reverse fault, I2R is expected to be in phase with V2. Fig. 5 shows I2R rotating in relation to V2 during the fault. This behavior causes the negative-sequence ground-fault directional element to initially declare the fault as forward (32GF) and then to change to reverse (32GR) later during the fault. Reference [3] provides more details on how this can lead to an undesired operation of the POTT scheme.

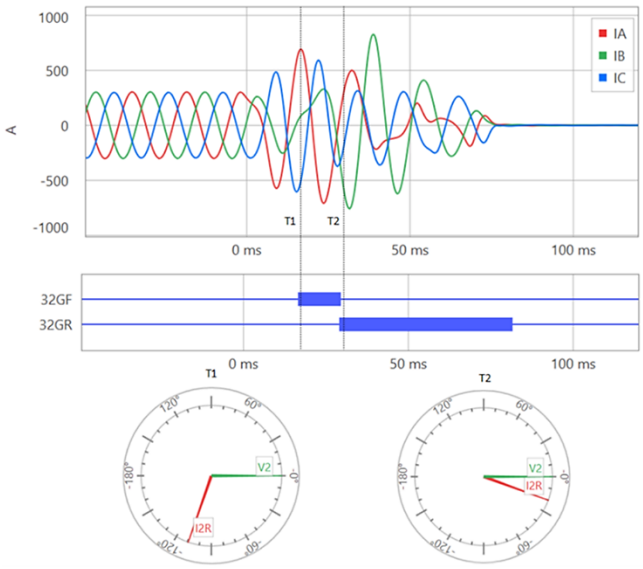

Fig. 5. Fault current and the relationship between I2R and V2 during the field fault.

Fig. 6 plots of the AG loop mho apparent impedance in the window between the orange and magenta time cursors. During the fault period, the apparent impedance has considerable variation. This varying behavior challenges both the underreaching and overreaching distance zones—creating security issues for instantaneous underreaching zones and dependability issues for overreaching zones used for step distance protection.

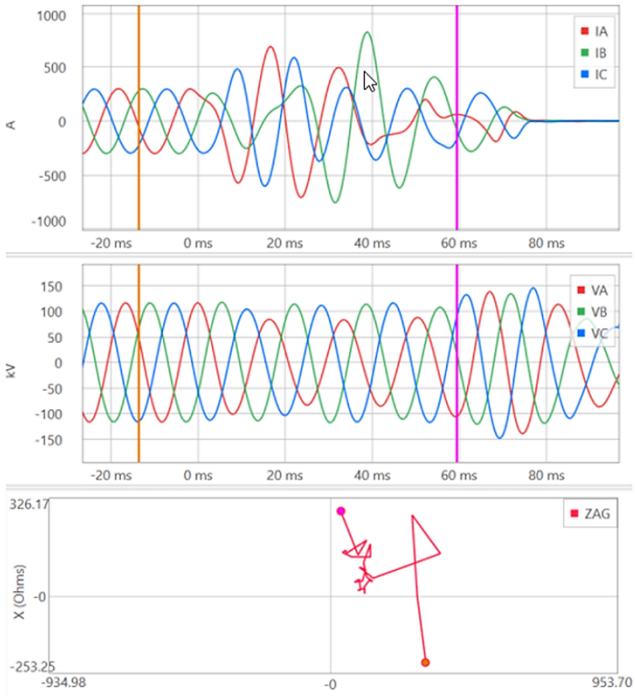

Fig. 6. AG loop mho apparent impedance.

Distorted current and voltage waveforms lead to phasor estimation errors, both in magnitude and angle. Fig. 7 shows that for the case under analysis, the heavy distortion on the current waveform caused errors in the magnitude and angle estimation, which resulted in a variation of the calculated apparent impedance. Note that positive-sequence memory voltage is the phasor angle referenced in Fig. 7.

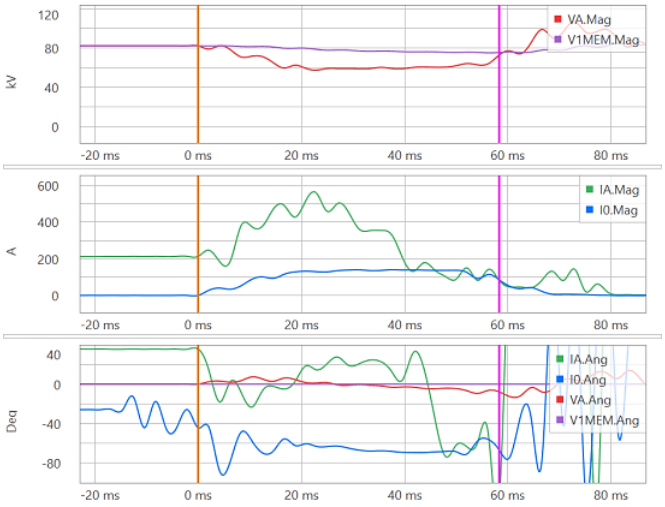

Fig. 7. AG loop mho phasor quantities magnitude and angle.

Fig. 8 shows the individual filtered phase (first three plots), negative-sequence (fourth plot), and zero-sequence (fifth plot) currents measured at each line terminal, as well as the respective differential current (DIA, DIB, DIC, DIG, and DIQ) calculated during the fault. The currents recorded at each terminal have the same magnitude and a 180 degree difference, resulting in zero differential.

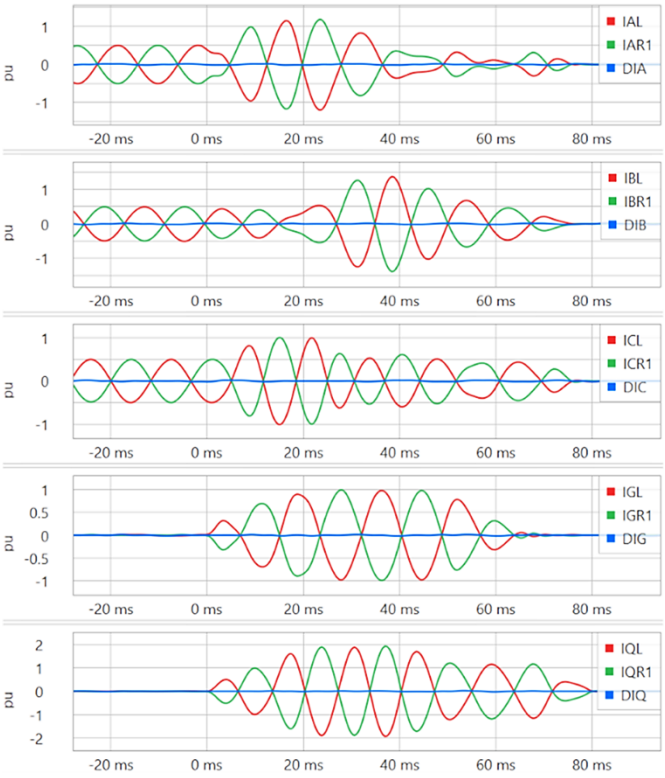

Fig. 8. Filtered phase, negative-sequence, and zero-sequence currents (in per unit) measured at each line terminal.

Despite the atypical behavior of the IBR, for external faults, its fault-current contribution passes through the line; therefore, it does not cause differential current in the phase, negative-sequence, or zero-sequence elements.

III. Transient-Based Protection Elements

Multifunctional ultra-high-speed (UHS) line protective relays are capable of implementing both phasor-based and transient-based protection elements [4]. Transient-based protection includes protection elements and schemes that are based on both incremental quantities (TD) and traveling waves (TW). These functions have shown to be applicable for the protection of transmission lines near unconventional sources, including IBR [3] [5] [6] [7]. Transient-based elements operate based on transients generated by the fault and are more independent of the source fault-current contribution.

Reference [8] introduces the fundamentals and operation principles of the time-domain directional element based on traveling waves (TW32), time-domain directional element based on incremental quantities (TD32), time-domain line differential element based on traveling waves (TW87), and time-domain distance element based on incremental quantities (TD21).

The TD21 element uses local current and voltage measurements to calculate the change in the instantaneous voltage at the reach point—this is the element operating quantity (VOP). The pre-fault voltage at the reach point establishes the maximum voltage change possible—this is the element restraining quantity (VRT). For faults beyond the reach point, the relay calculates VOP lower than VRT. For faults shorter than the reach point, the relay calculates VOP greater than VRT.

The TW87 scheme uses the relative arrival time, polarity, and magnitude of current TWs (at local and remote terminals) to determine whether the fault occurred on the protected line. Due to the CT polarity, TWs observed, both at the local and remote terminals, have the same polarity and are separated by less than the TW line propagation time for internal line faults. In addition, the UHS relay calculates operating and restraining quantities based on the measured current TW at both line terminals and compares these quantities to make a trip decision.

To determine the fault direction, the TW32 element uses relative polarity of the first voltage and current TWs that travel from the fault to the relay location. A line fault launches current and voltage TWs toward the relay from the fault point, which results in voltage and current TWs with opposite polarities due to the line-protection CT polarity. For a reverse fault, the relay measures voltage and current TWs with the same polarities.

The TD32 element operates based on the incremental voltage (Δv) and the incremental replica current (ΔiZ). For a forward fault, the relationship between Δv and ΔiZ is the negative of the absolute value of the source impedance behind the relay (ZS). For a reverse fault, the relationship between Δv and ΔiZ is the absolute value of the sum of the protected line impedance (ZL) and the source impedance of the remote terminal (ZR).

The fact that Δv and ΔiZ will have opposite polarities for forward faults and matching polarities for reverse faults will always be true, because the circuit behind the relay for forward faults and the circuit in front of the relay for reverse faults is inductive. After a fault in the network, the IBR control takes time to act [9]. Therefore, at least in the first milliseconds, the IBR behaves as a passive element. Reference [6] demonstrates that the IBR equivalent impedance is mostly inductive during the first milliseconds after a fault, which allows for the reliable application of the TD32 element to determine the fault direction.

A. *Communication Requirements*

TW32 and TD32 are UHS directional elements that are associated with permissive or blocking directional comparison pilot protection schemes. These elements are applied over standard analog or digital pilot protection channels, including contact digital input and output, low-bandwidth (64 kbps) multiplexed communication channels, direct-fiber-optic channels, or any combination of these.

The TW87 element needs real-time exchanges of 1 MHz sample voltages and currents between the two terminals of the line. It requires high-bandwidth (1 Gbps) protection signaling with jitter below 25 ns and asymmetry below 100 ns. These requirements are met with direct-fiber-optic channel or wavelength division multiplexing, such as dense wavelength division multiplexing.

B. *Transmission Lines Terminated With Only Power Transformers*

Transmission line faults launch voltage and current TWs that propagate toward the line terminals. When an incident wave (i_I) reaches the line terminal, part of the wave is transmitted (i_T) and part of the wave is reflected (i_R), as shown in Fig. 9.

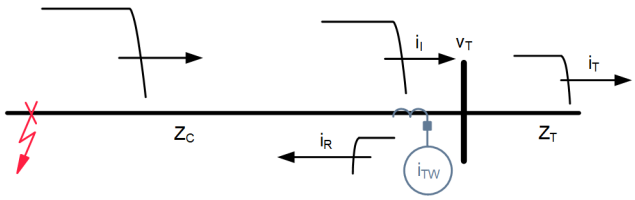

Fig. 9. Representation of incident (i_I), reflected (i_R), and transmitted (i_T) waves at a transmission line terminal.

The portion of the wave that is reflected depends on the relationship between the characteristic impedance (Z_C) of the line and the equivalent termination characteristic impedance (Z_T), which can be determined using **Error! Bookmark not defined.**(1).

$$i_R = \frac{Z_C - Z_T}{Z_C - Z_T} i_I \quad (1)$$

A relay that measures the TW current signal at the line terminal sees the sum of the incident and the reflected currents (i_{TW}) according to (2).

$$i_{TW} = i_I + i_R \quad (2)$$

Some IBRs are radially connected to the grid, as with the example IBR shown on the simplified diagram in Fig. 2. When

a line is terminated with a high-characteristic (surge) impedance, such as with only power transformer, Z_T has a much higher value compared to Z_C. This causes i_R and i_I to have opposite polarities and results in an i_{TW} with a lower magnitude than the incident wave. The dependability of the TW87 element is compromised due to the low TW current at the line end terminating on the transformer [10]. Alternatively, [10] introduces the concepts and operational details of the time-domain overcurrent element based on traveling waves (TW50). It takes advantage of the high-impedance termination of the power transformer, which does not allow the propagation of TWs with significant magnitude through the transformer.

IV. The Utility's Standard Protection Solution

Since 2016, the utility has developed several wind farms and PV plants across the country, with nearly 2,000 MW of installed capacity. These projects typically consist of numerous wind turbines or PV generators connected by a medium-voltage network to a collector substation. At the substation, one or more step-up power transformers are installed, and the generated energy is then connected to the Brazilian bulk power system (GRID) via a high or extra-high voltage transmission line, as illustrated in Fig. 10.

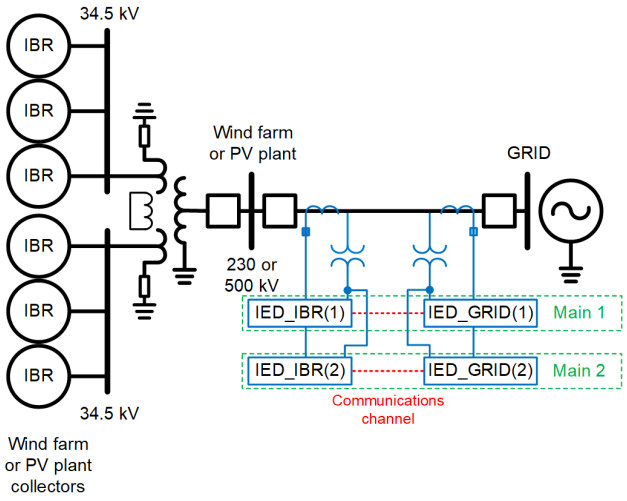

Fig. 10. Simplified one-line diagram of a typical wind farm or PV plant, its connection to the grid transmission network, and the transmission line protective IEDs.

In the initial projects, the transmission line-protection system was composed of redundant traditional phasor-based (PB) relays—Main 1 and Main 2—both from the same manufacturer and model, in accordance with the minimum requirements defined in Brazil by the National Electric System Operator [11].

After encountering unsatisfactory performance of the protection system during electrical system events, as discussed in Section II of this paper, the utility's technical team initiated research to seek alternative solutions for enhancing the safety and reliability of protection schemes for future projects.

It is important to note that the protection solution must be optimized for diverse operating conditions, as the utility employs different types of IBRs, including:

- PV solar systems
- Wind turbines:
  - Type 3: doubly-fed induction generator (DFIG)
  - Type 4: full converter

Numerous technical papers have been published and widely discussed in past workshops, seminars, and conferences, analyzing the impact of integrating IBRs into the power system, and on the performance of traditional protective relay functions. This body of literature not only highlights the challenges but also proposes solutions [1], including particular setting calculations for PB protection elements in systems with IBRs to keep these elements safe and reliable [12].

The incorporation of transient-based protection functions was also considered highly important for reliable protection schemes, as these functions rely on fault-induced transients and are therefore less dependent on energy-source characteristics [13].

As a result of this research, the utility decided to adopt a hybrid approach, combining the strengths of both transient-based and PB protective relays as the standard protection solution for upcoming projects.

A. Pilot Line Protection

Pilot protection functions depend on the availability of a reliable communications channel. Therefore, we recommend establishing two independent communication paths—one per protective relay (Main 1 and Main 2). Because most of the overhead transmission lines are typically shorter than 40 km (25 miles), using optical ground wire (OPGW) and directly connecting the fiber-optic channel between the protective relays is a suitable solution for transferring signals between both ends of the line. To meet the requirement for dual communication paths, installing OPGW on both ground wires is currently the most economical option.

There are exceptions where transmission lines exceed the reach of the optical ports of the IEDs. In such cases, a redundant IEEE Std C37.94 network is implemented instead.

Applied protection functions:

- Main 1 protective relay (UHS relay)
  - Line differential element based on traveling waves (TW87)
  - Permissive overreach transfer-trip scheme with:
    - Time-domain directional element based on traveling waves (TW32)
    - Time-domain directional element based on incremental quantities (TD32)
    - PB distance element (21), phase and ground, including echo and weak-infeed logic
    - PB ground directional overcurrent element (67G), including echo and weak-infeed logic
- Main 2 protective relay (PB relay)
  - Phase, negative-sequence, and zero-sequence line current differential elements (87LA, 87LB, 87LC, 87LQ, and 87LG)
  - Permissive overreach transfer-trip scheme with:
    - Distance element (21), phase and ground, including echo and weak-infeed logic

- Ground directional overcurrent element (67G), including echo and weak-infeed logic
- Ground directional control is automatically selected from: negative-sequence impedance (32Q) or zero-sequence impedance (32V)

Considering this group of protection functions, the PB line current differential protection is the least affected by the presence of IBRs in the system. Nevertheless, we recommend enhancing security, particularly for elements that rely on negative-sequence currents [12], as these quantities are less reliable when nonconventional sources are subjected to faults in the power system. PB directional elements, which also supervise PB distance elements in the Main 2 protective relay, are configured to operate only when the source is the connected to the grid, where fault-current contributions originate from systems with a higher penetration of synchronous machines, thereby ensuring greater security. Because protection elements on the IBR side exhibit reduced sensitivity, complementary logics, such as echo, weak infeed, and time-delayed undervoltage functions, are employed to ensure breaker tripping.

Transient-based protection functions are generally configured without requiring special adjustments for the presence of IBRs.

B. Distance and Step Distance Protection

- Main 1 protective relay (UHS relay)
  - Time-domain distance element based on incremental quantities (TD21)
  - PB distance, phase and ground, Zone 1, instantaneous elements
  - PB step distance, phase and ground, Zone 2, time-delay elements
- Main 2 protective relay (PB relay)
  - Distance, phase and ground, Zone 1, instantaneous elements
  - Step Distance, phase and ground, Zone 2, time-delay elements

The same considerations apply to protection functions that operate with the aid of teleprotection. That is, in faults fed by the IBR, it is important to avoid the operation of protection elements that rely on the conventional behavior of symmetrical components during the oscillatory phase of the apparent impedance. For the Zone 1 distance protection, a slight time delay helps prevent overreach. Directionality errors by the 32Q or 32V elements can be mitigated by increasing the minimum current thresholds that enable the directional function (setting strategies are detailed in [12]).

C. Ground Time Directional Overcurrent Protection

- Main 1 protective relay (UHS relay)
- Main 2 protective relay (PB relay)

The ground directional time overcurrent element is backup protection for phase-to-ground faults that can be set with an sensitive pickup current, thus providing good coverage for high-impedance faults. The contribution current, even on the IBR side, originates from the power system, since the step-up transformer at the collector substation has a grounded wye winding on the extra-high voltage side, providing a path for the fault-current contribution. Additionally, there will always be a delta winding in the transformer to compensate for ampere-turns, see Fig. 10.

The time dial of the inverse-time curve should be selected to coordinate with Zone 2 of the other transmission lines at the connection substation.

D. Phase and Ground Time Emergency Overcurrent Protection

- Main 1 protective relay (UHS relay)
- Main 2 protective relay (PB relay)

Phase and ground non-directional time overcurrent emergency elements are activated only when the following two conditions occur simultaneously: there is a loss of potential from the line VT, and the current-based pilot protection is out of service on both the Main 1 and the Main 2 relays.

V. Field Cases Analysis

In this section, we present the analysis for the performance of the transient-based elements and PB protection elements, for internal and external faults, from devices applied in the transmission lines connecting IBRs to the grid. The traveling-wave-based differential scheme is not included in our analysis since its dependability is compromised due to the low TW current at the line end terminating on a transformer, as previously mentioned.

A. Case 1: Internal Phase-C-to-Ground Fault 500 kV Line, Wind Farm 1

The first field case analysis discusses an internal single-line-to-ground (SLG) fault on a 500 kV line that connects a wind farm to the grid.

Fig. 11 shows the simplified one-line diagram of the system for Case Analysis 1.

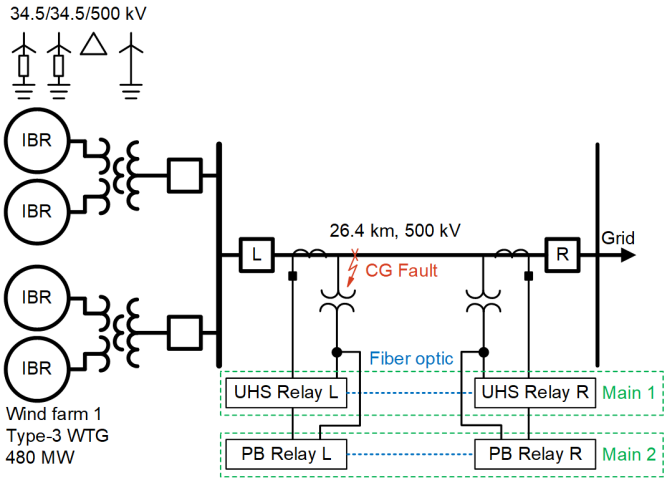

Fig. 11. One-line diagram for Field Case Analysis 1.

The wind farm for this case analysis has 85 type-3 wind turbine generators, distributed between two medium-voltage 34.5 kV busbars. The total capacity for this wind farm is 480 MW, and it connects to the grid through a 500 kV line with a total length of 26.4 km.

The line-protection scheme consists of two protective relays, the Main 1 Relay (the UHS Relay L and the UHS Relay R shown in Fig. 11) is a multifunctional device with transient-based protection elements (as described in Section III) and enhanced PB protection elements, which includes distance (21) and directional (67) elements. The Main 2 Relay (the PB Relay L and the PB Relay R shown in Fig. 11) is a multifunctional device with PB protection elements, which includes line differential (87L), distance (21), and directional (67) elements. The PB protection elements were configured according to the recommendations from [12].

Both schemes have direct-fiber communications to implement pilot schemes, which include line differential and POTT schemes. Such an approach with dedicated fiber-optic channels removes the need for external time synchronization to align samples from local and remote relays for the 87L element, making the protection scheme more reliable and independent from additional devices [14].

The wind farm is connected to the 500 kV system through four winding transformers. It has a buried delta-connected winding, and the 500 kV winding for the farm is wye-connected and solid grounded, which provides a path for the zero-sequence current.

The 500 kV experienced an SLG fault, CG, at 1.6 km from the wind farm terminal, while generating 133 MW at a power factor equal to 0.99.

Fig. 12 shows the oscillography captured during the CG fault by the relays from terminals L and R, on the wind farm side and the grid side, respectively.

As expected, the fault-current contribution from the wind farm is much lower than the fault-current contribution from the grid, even for this event, where the fault is close to the wind farm in Fig. 11.

The fault current on Phase-C, from the wind farm terminal (ICL), was cleared in 30.2 ms (1.81 cycles, 60 Hz system) from the fault inception and for the grid terminal (ICR), in 32.8 ms (1.97 cycles), as shown in Fig. 12. Basically, this is the circuit breaker total operating time. The extremely fast current interruption was due to the performance of the UHS relay.

Analyzing the event reports generated by the UHS Relay L (Fig. 13) and the UHS Relay R (Fig. 14) reveals that the short-fault-clearing time was the result of the high-speed operation of the time-domain directional element based on incremental quantities (TD32) and the fast processing of the communications by the relays associated with the POTT scheme. With direct fiber providing fast communications, the permissive signal keyed by the TD32 element, the element detecting a forward fault (i.e., TD32F), was received in 0.1 ms by the remote UHS relay, and the TD32 element operation time was 2.2 ms, allowing the fault to be cleared in less than 2 cycles by both terminals of the transmission line.

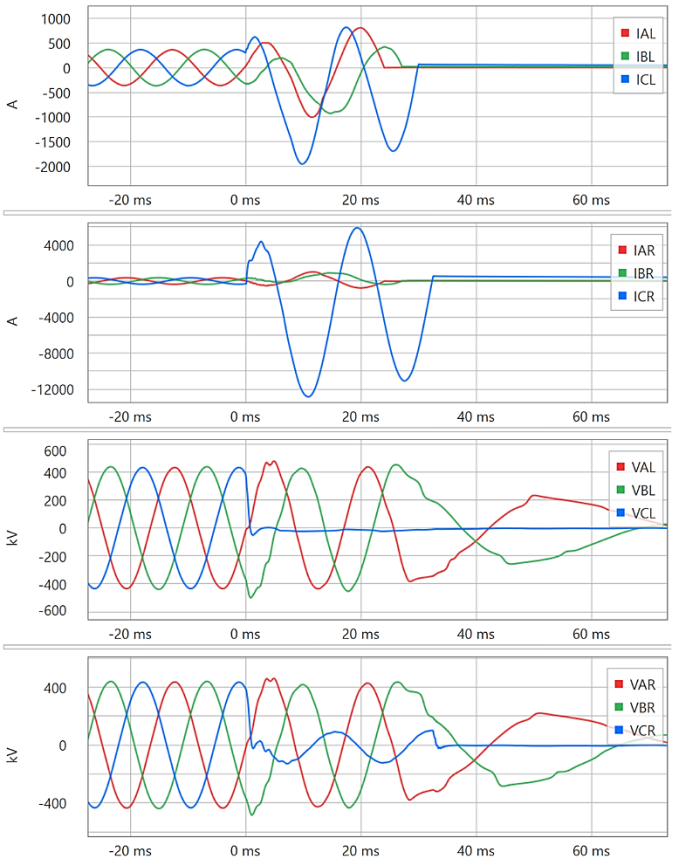

Fig. 12. Voltages and currents from Terminal L, wind farm side, and Terminal R, grid side, for the CG fault.

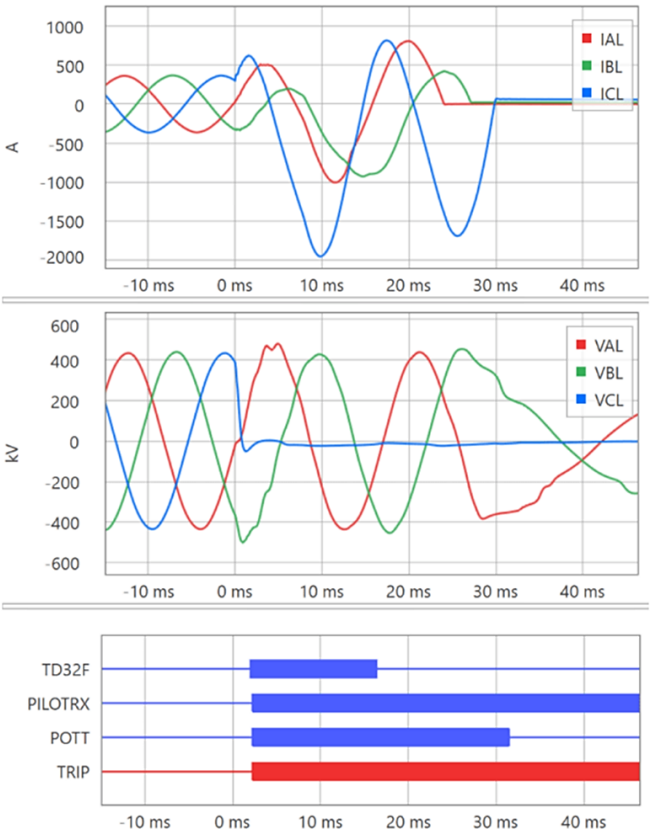

Fig. 13. Case 1 event report from UHS Relay L for the CG fault shows the operation of the TD32F element in 2.2 ms after fault inception.

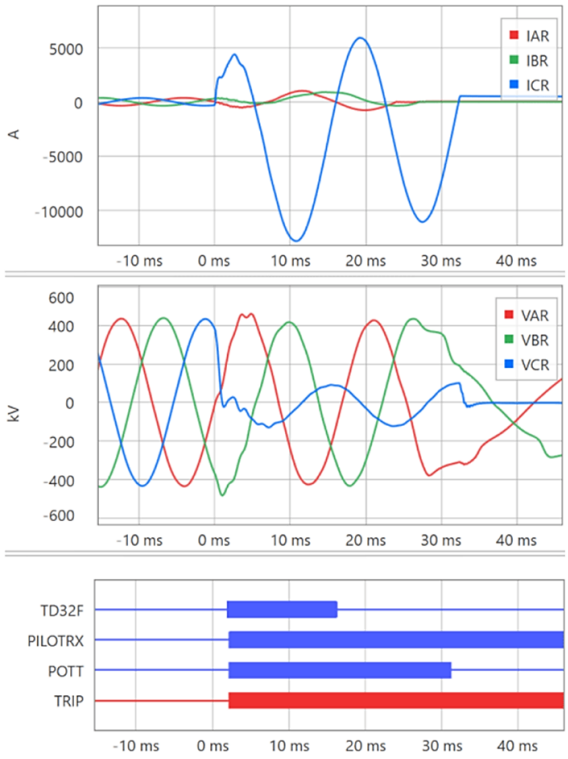

Fig. 14. Case 1 event report from UHS Relay R for the CG fault shows the operation of the TD32F element in 2.2 ms after fault inception.

The event reports generated by the PB Relay L (Fig. 15) and PB Relay R (Fig. 16) show that the Phase-C PB line differential element operated in 17.5 ms.

Line differential protection is, in general, a natural choice for lines connecting IBRs to the grid, because it is secure and dependable. The time-domain directional elements based on incremental quantities, implemented in the PB Relay, are secure and dependable as well [15]. These elements have the advantage of being much faster and can be implemented with low-bandwidth communications channels, like a power line carrier.

The PB relay includes a high-speed directional element based on incremental quantities in the frequency domain [16]. The forward declaration of the high-speed ground directional element is identified (Fig. 15 and Fig. 16) by the HSDGF element, which in association with a PB overcurrent element (F32QG) creates the 67G2 element to be used in the POTT scheme. The 67G2 element keys the POTT permissive signal to be sent to the remote terminal and in association with the permissive trip (PT) signal received from the remote terminal, may create a trip by the POTT scheme (COMPRM) if certain requirements are fulfilled, which then trips the circuit breaker (TRIP). For this specific event, the FHSDG element was efficient and notably quick in detecting the CG fault from the IBR side (13 ms) and grid side (7 ms). The PB negative-sequence element (F32QG) was configured according to [12], which recommends setting the overcurrent supervision higher than the maximum contribution from the IBR, essentially defeating the element for forward faults and releasing it only for a reverse fault on the IBR side to block the echo or weak-infeed operation for the POTT scheme. Fig. 15 shows that the F32QG element didn't pick up for this fault as expected. The element picked up during the circuit-breaker operation due to the non-simultaneous current interruption of the phases. The F32QG element from the grid side operated in 17 ms—simultaneously with the line-differential-element operation.

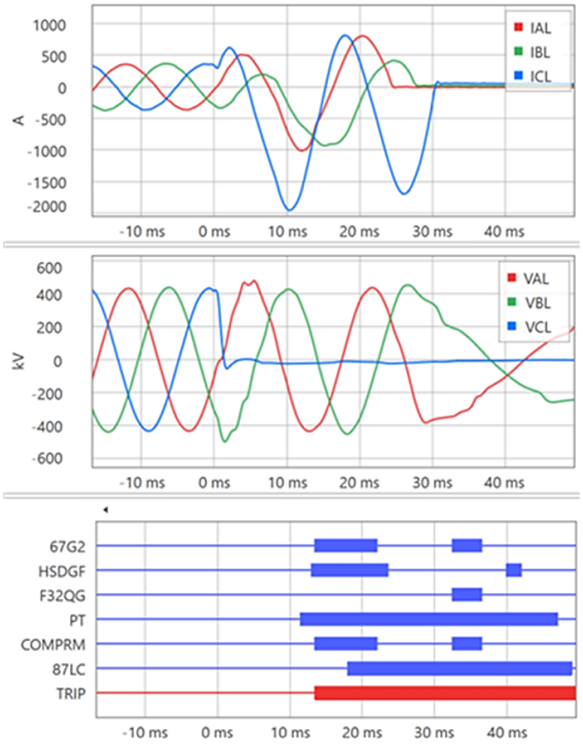

Fig. 15. Case 1 event report from PB Relay L for the CG fault shows the operation of the 87LC element in 17 ms after fault inception.

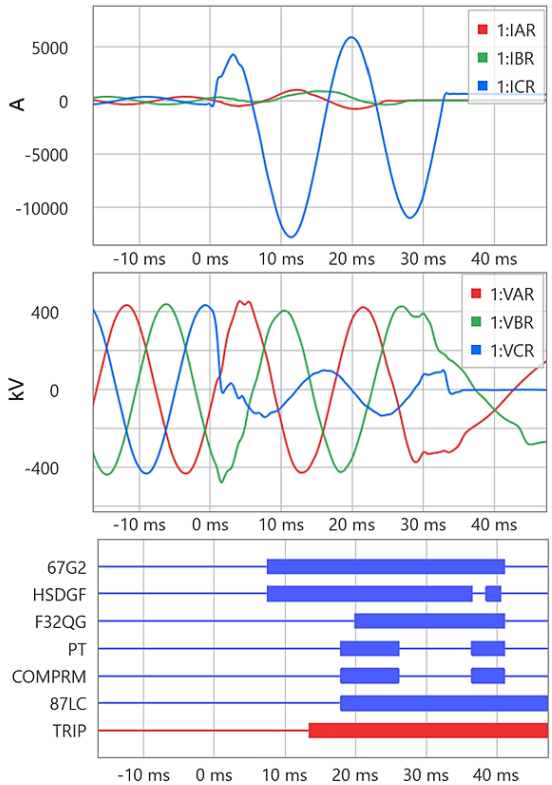

Fig. 16. Case 1 event report from PB Relay R for the CG fault shows the operation of the 87LC element in 17 ms after fault inception.

In the case that the HSDGF element and the F32QG element from the L terminal do not operate for an internal fault in the transmission line, the weak infeed and echo logic associated with the POTT scheme will trip the wind farm terminal.

B. Case 2: Internal CG Fault 500 kV Line, Wind Farm 2

Field Case Analysis 2 discusses an internal SLG fault on a 500 kV line that connects the wind farms to the grid.

Fig. 17 shows the simplified one-line diagram of the system for Case Analysis 2.

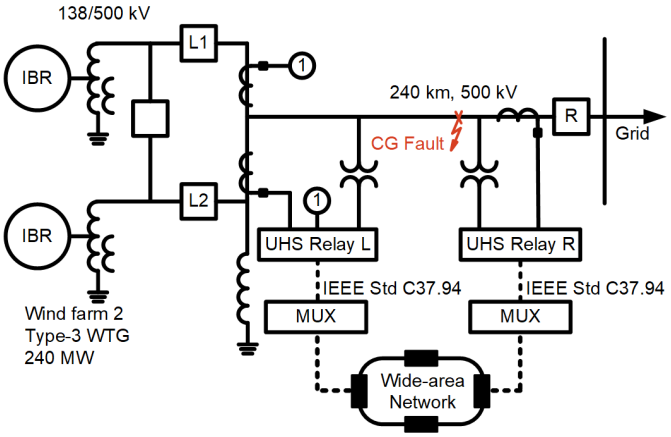

Fig. 17. One-line diagram for field Case Analysis 2.

The total capacity for the wind farms is 240 MW, and it is connected to the grid through a 500 kV line with a total length of 240 km.

The UHS relays, shown in Fig. 17, are installed to provide traveling-wave-based fault location (TWFL) and to pilot, and gain experience with, transient-based protection elements (the UHS relays were not actually tripping the circuit breakers when the fault discussed in this section happened). The line-protection scheme (which is not the scheme shown in Fig. 17) consists of two PB protective relays at each line terminal.

In this case analysis, there is no direct fiber to provide communications between the two UHS relays, as there was for the previous case. The communications channel was established through multiplexers with IEEE Std C37.94 protocol, which allows the implementation of the double-ended TWFL and POTT schemes.

The wind farm connects to the 500 kV system through autotransformers, and the autotransformers have a delta-connected tertiary winding, which provides a path for the zero-sequence current.

Fig. 18 and Fig. 19 show the oscillography captured for the CG fault (shown in Fig. 17) by the wind farm side terminal (UHS Relay L) and grid-side terminal (UHS Relay R), respectively.

Fig. 18 shows that the fault was cleared 48.9 ms on the wind farm side terminal. The same figure shows that the TD32F element operated in 1.3 ms and the circuit-breaker trip logic (TRIP) operated in 4.1 ms, as soon as the POTT permissive signal—keyed by the time-domain directional element based on traveling waves (TW32F)—was received. However, as already mentioned, the UHS relay was not wired to trip the circuit breaker, which means the electrical power system did not benefit from the UHS relay fast operation.

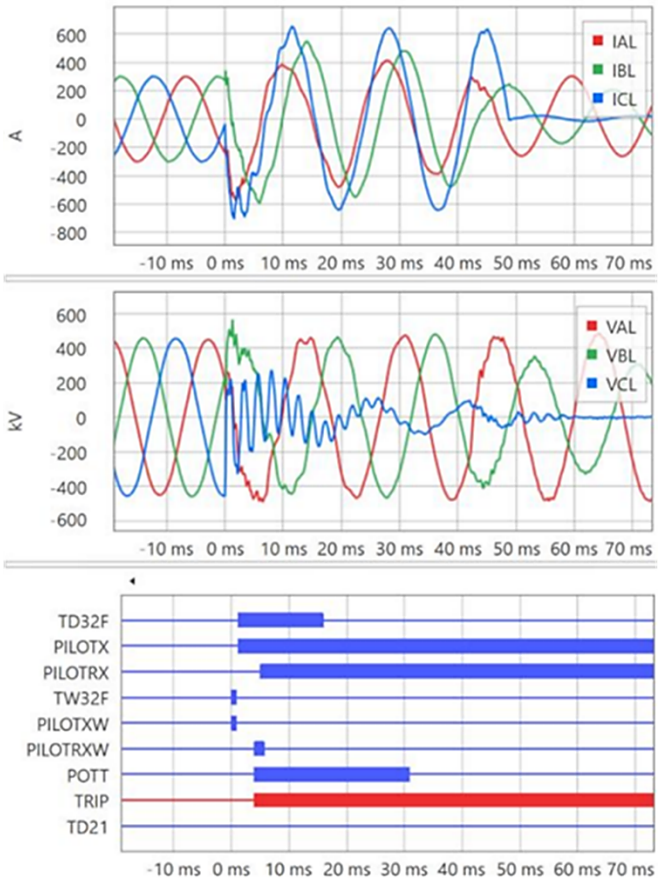

Fig. 18. Case 2 event report from UHS Relay L for the CG fault shows the operation of the TD32F and TW32F elements in 1.3 ms and 0.1 ms after fault inception, respectively.

The TW32F element is intended to be used with a low-latency communications channel, such as a direct-fiber-optic channel, to provide a faster trip by the POTT scheme. The application for Wind Farm 2 does not have a direct-fiber channel, but this case analysis shows that the protection scheme may benefit from the use of the TW32F element, even with the multiplexed IEEE Std C37.94 channel. The TW32F element from the grid-side terminal (UHS Relay R) operated in 0.1 ms (Fig. 19), which keyed the POTT permission that was sent through the IEEE Std C37.94 channel to UHS Relay L. Relay L received the POTT permissive signal keyed by the TW32F element (PILOTRXW) 4 ms later. The received permission to trip (PILOTRX) signal, which is keyed by the TD32F element, arrived at 5.1 ms—1 ms later than PILOTRXW. This case demonstrates that the use of the TW32F element can accelerate POTT tripping by about 1.0 to 2.0 ms compared with only applying the TD32F element for keying the POTT permission.

If UHS Relay L was wired to trip the circuit breaker, the total fault clearing time could be reduced from 48.9 ms to about 30 ms for this event, in other words the circuit-breaker interruption time added to the time for next current zero-crossing, given how fast the UHS relay is.

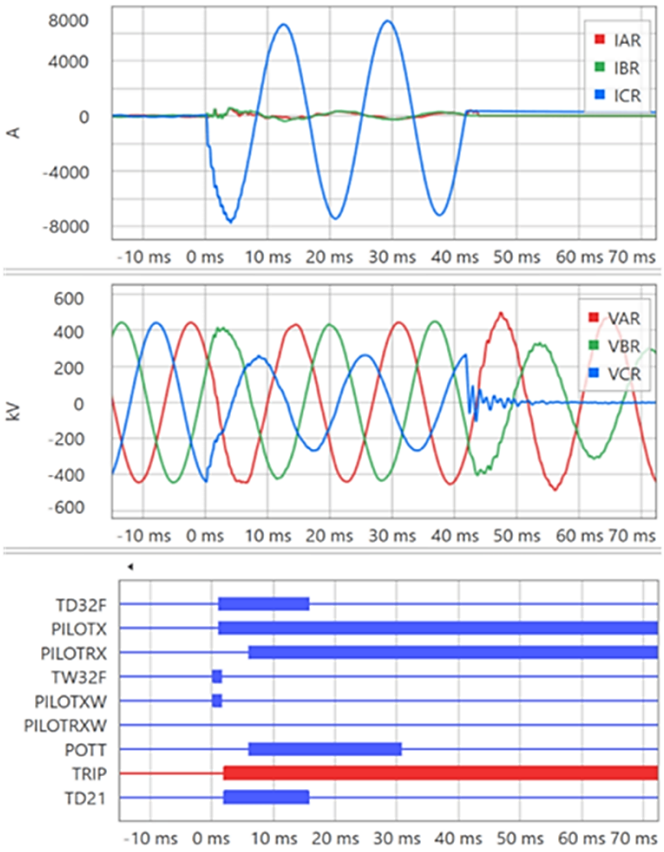

Fig. 19. Case 2 event report from UHS Relay R for the CG fault shows the operation of the TD32F and TW32F elements in 1.0 ms and 0.1 ms after fault inception, respectively.

For the grid-side terminal, UHS Relay R—the time-domain distance element based on incremental quantities (TD21)—operated in 1.8 ms after fault inception (as shown in Fig. 19) and asserted TRIP at the same time; meaning, that if this relay was wired to trip the circuit breaker, the total fault clearing time could be reduced from 42.5 ms to about 25 ms, in other words the circuit-breaker interruption time added to the time for next current zero-crossing, given how fast is the UHS relay.

Fig. 19 shows that the PILOTRXW didn't pick up. The PILOTRXW didn't pick up because the TW32F element, from UHS Relay L, remained asserted for a significantly short period—0.6 ms. This was because the relay detected an electromagnetic interference condition in local currents that may have jeopardized the security of the TW-based protection; furthermore, the short duration of the signal received by UHS Relay R was not validated by the secure check to use the signal (received through the IEEE Std C37.94 channel) in the trip decision. For comparison, the TW32F element asserted for 1.2 ms at Relay R, which was sufficiently long to satisfy the security counts at Relay L and to assert PILOTRXW. As mentioned earlier, the application of the TW32F element to accelerate the trip by the POTT scheme is more efficient with the use of a direct-fiber-optic channel, as will be demonstrated in the analysis of Case 3.

C. Case 3: Internal AG Fault 500 kV Line, Wind Farm 3

Field Case Analysis 3 discusses an internal SLG fault on the 500 kV line that connects Wind Farm 3 to the grid.

Fig. 20 shows the simplified one-line diagram of the system for Case Analysis 3.

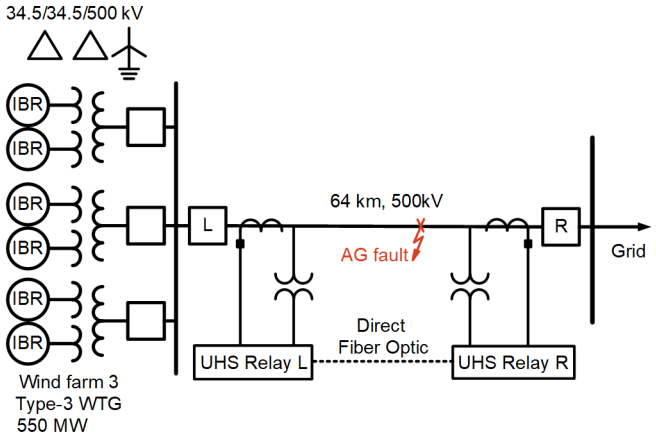

Fig. 20. One-line diagram for Field Case Analysis 2.

The total capacity for the wind farm is 550 MW, and it is connected to the grid through a 500 kV line with a total length of 64 km.

The UHS relays (shown in Fig. 20) were installed to provide TWFL and to pilot, and gain experience with, transient-based protection elements (UHS R and L were not actually tripping the circuit breakers when the fault discussed in this section happened). As with Case Analysis 2 (discussed in the previous section), the line-protection scheme for this case (not the scheme shown in Fig. 20) consists of two PB protective relays at each line terminal.

The UHS relays have direct-fiber communications to implement the POTT and the double-ended TWFL schemes.

In Case Analysis 3, the wind farm is connected to the 500 kV system through three winding transformers, with the 34.5 kV windings connected in delta, and the 500 kV winding being wye-connected and solid grounded, which provides a relatively low-impedance path for the zero-sequence current.

And the 500 kV experienced an SLG AG fault at 47 km from the wind farm terminal.

Fig. 21 and Fig. 22 show the oscillography captured for the AG fault (shown in Fig. 20) by the wind farm side terminal (UHS Relay L) and grid-side terminal (UHS Relay R) respectively.

Fig. 21, shows that, as expected, the wind farm terminal contributes almost exclusively with the zero-sequence current to the fault because of the relatively low zero-sequence of the step-up transformers.

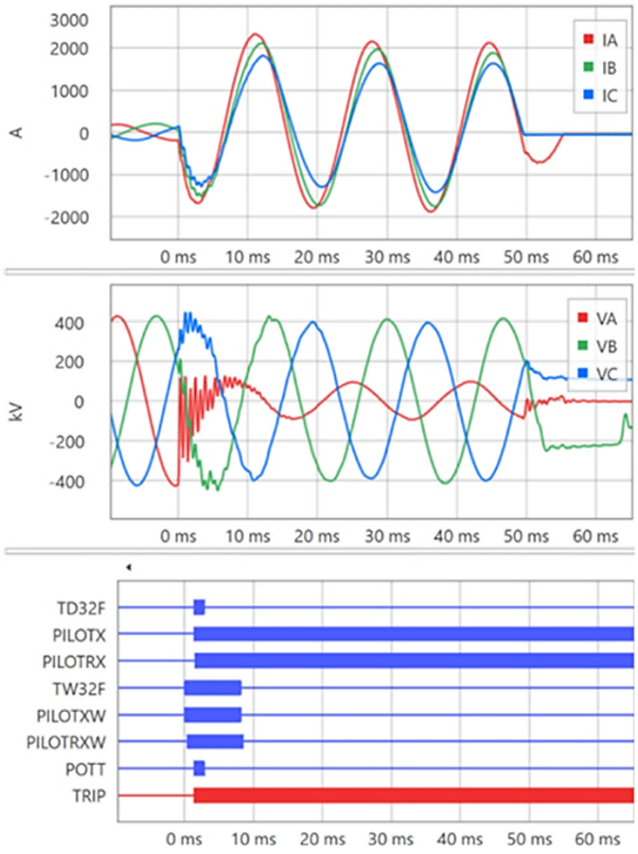

Fig. 21. Case 3 event report from UHS Relay L for the AG fault shows the operation of the TD32F and TW32F elements in 1.4 ms and 0.1 ms after fault inception, respectively.

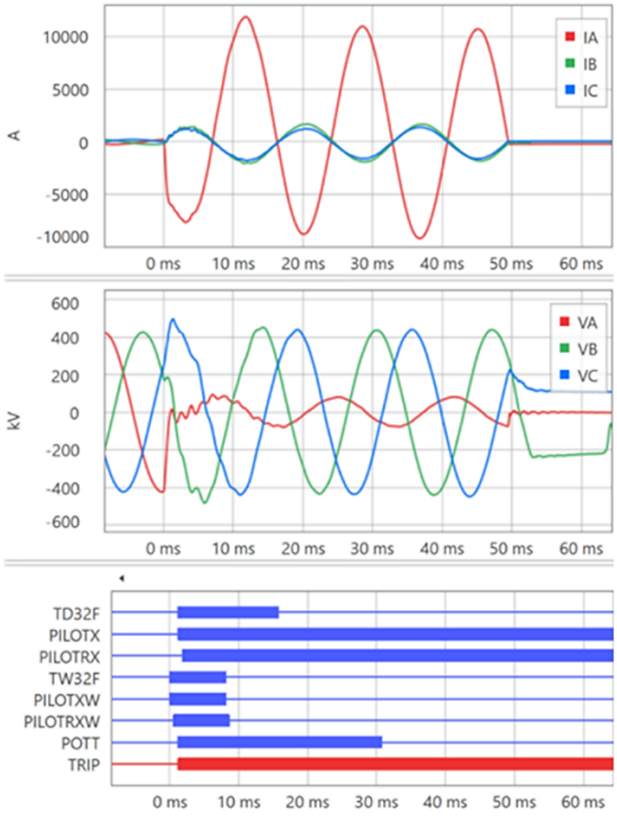

Fig. 22. Case 3 event report from UHS Relay R for the AG fault shows the operation of the TD32F and TW32F elements in 1.3 ms and 0.1 ms after fault inception, respectively.

Fig. 22 shows that the fault was cleared in 49.1 ms on the grid-side terminal because the transient-based protective relays were not tripping the circuit breaker at that time. For this application, for which the direct-fiber channel is available, the TRIP asserted at 1.3 ms. The PILOTRXW permissive signal was received at 0.6 ms. The breaker could be tripped as soon as the TD32F element operated at 1.3 ms, and the fault could be cleared in 25 ms. If the TW32F element was not used in the POTT scheme, the digital POTT and TRIP would be asserted in 2 ms, when the permissive signal PILOTRX was received by UHS Relay R.

A similar sequence happened for the wind farm terminal side, and the TRIP asserted in 1.4 ms after the fault inception.

The Phase-A current (IA) from the wind farm side terminal is not interrupted at the same time that the currents from Phases-B (IB) and Phase-C (IC) are; the phase current is interrupted 6 ms later. As the three currents are basically in phase, one can expect that they should be interrupted at the same zero-crossing. This may be an indication that something abnormal happened for Phase-A. The UHS relays provide ultra-high-resolution transient recordings with a sampling rate of one million samples per second. The ultra-high-resolution recording for IA is shown in Fig. 23 and the detailed view (highlighted by the black square) is shown in Fig. 24, proving that IA was interrupted at 49.1 ms and reignited 0.2 ms later.

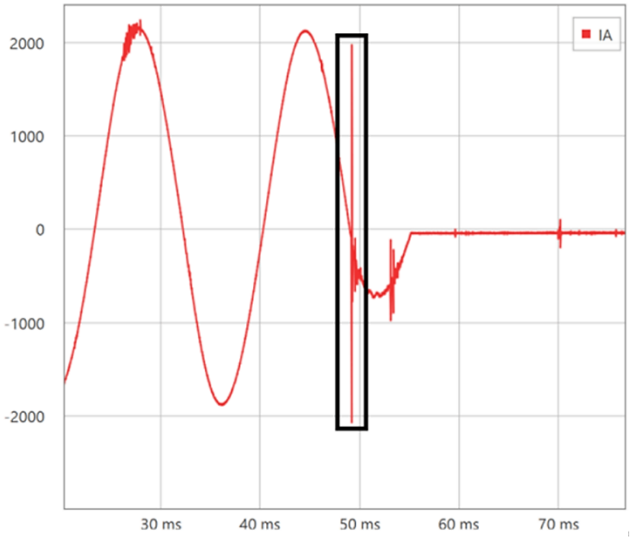

Fig. 23. Ultra-high-resolution recording for IA current.

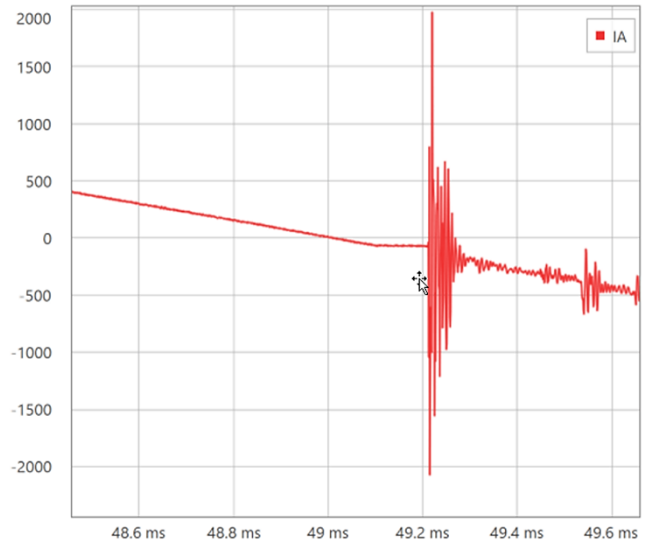

Fig. 24. Reignition in the IA current.

D. Case 4: External BC Fault 500 kV System, Wind Farm 3

Field Case Analysis 4 discusses an external phase-to-phase (Phase-B and Phase-C) fault where Wind Farm 3 (from the previous section) connects to the 500 kV grid (Fig. 20). This fault is forward for the UHS Relay L and reverse for UHS Relay R.

Fig. 25 shows the event report captured by UHS Relay R, grid side. As expected, the external fault was detected as reverse. The time-domain reverse directional element based on incremental quantities (TD32R) and the time-domain reverse directional element based on traveling waves (TW32R) operated in 9.0 ms and 0.1 ms, respectively. The TD32R element asserted the current reversal logic (REV_BLK), which supervises and, for security, temporarily blocks the POTT trip during the clearing of a fault on a parallel line. The transient-based elements arming logic (ARMED) deasserted 1.0 cycle after the fault inception and asserted again 1.5 cycles after the external fault was cleared, bringing the transient-based element in-service again. The arming logic verifies quiescent system conditions to ensure secure operation of the transient-based protection elements. The UHS relay inhibits operation of the transient-based protection elements if the arming logic is not asserted. The purpose of the arming logic is to verify that the protected line is energized and that there are no excessive transients prior to a fault

The TR Relay L (on the IBR side) did not pick up for this external BC fault because the fault current was not enough to allow the forward directional element to operate. This demonstrates that the reverse transient-based directional element is more sensitive than the forward directional element, as it must be in a POTT pilot protection scheme.

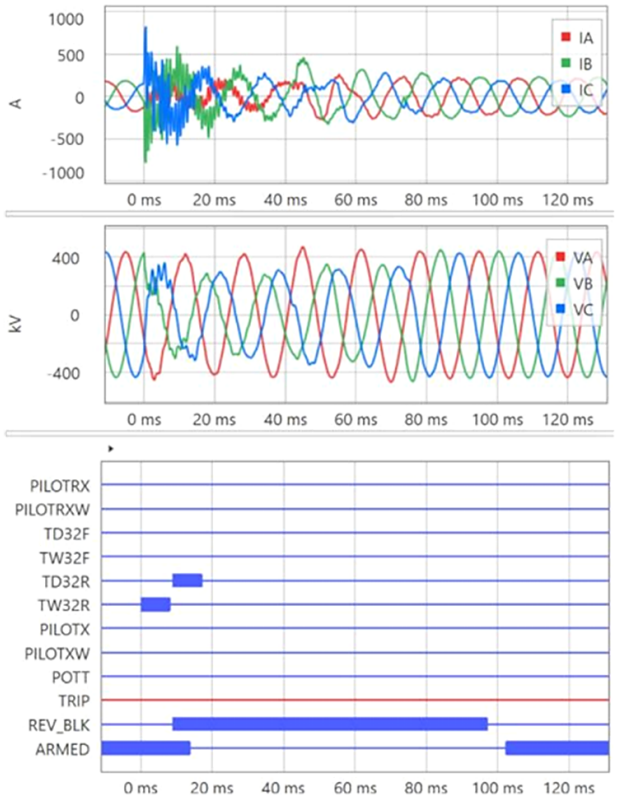

Fig. 25. Case 4 event report from UHS Relay R for the BC external fault shows the operation of the TD32R and TW32R elements in 9.0 ms and 0.1 ms after fault inception, respectively.

VI. Conclusion

Our paper demonstrates that transient-based line-protection elements, when applied for pilot protection schemes, are extremely dependable and secure when compared to PB elements and schemes in systems with renewable energy sources. The results of the field-event analyses we present in this paper indicate that the adoption of time-domain-based protection functions significantly enhances the reliability of power system operations, especially in scenarios with a high penetration of renewable sources. The implementation of these technologies represents an important step towards the modernization of transmission networks, and the efficient integration of renewable energy sources.

The utility's standard for transmission lines, which applies PB line current differential relays and transient-based relays, has proved to be an excellent choice amid the increasing expansion and adoption of renewable energy sources.

VII. References

[1] R. Chowdhury and N. Fischer, "Transmission Line Protection for Systems With Inverter-Based Resources—Part II: Solutions," proceedings of the IEEE Transactions on Power Delivery, Virtual Format, October 2020. Available: ieeexplore.ieee.org/document/9233925.

[2] D. Costello and K. Zimmerman, "Determining the Faulted Phase," proceedings of the 36th Annual Western Protective Relay Conference, Spokane, WA, October 2009.

[3] M. Bini, P. Lima, and F. Lollo, "Challenges and Solutions in the Protection of Transmission Lines Connecting Nonconventional Power Sources," proceedings of the 48th Annual Western Protective Relay Conference, Spokane, WA, October 2021.

[4] SEL-T401L Ultra-High-Speed Line Relay Instruction Manual. Available: selinc.com.

[5] B. Kasztenny, "Short-Circuit Protection in Networks With Unconventional Power Sources," *PACW Magazine*, March 2021.

[6] B. Kasztenny, "Line Protective Relays Suitable for Systems With a High Penetration of Unconventional Sources—Operating Principles and Field Experience," for presentation at CIGRE, Cairns, AU, 2023, in press.

[7] B. Kasztenny, "Distance Elements for Line Protection Applications Near Unconventional Sources," Original edition released June 2021.

[8] E. O. Schweitzer, B. Kasztenny, A. Guzmán, V. Skendzic, and M. V. Mynam, "Speed of Line Protection—Can We Break Free of Phasor Limitations?" proceedings of the 68th Annual Conference for Protective Relay Engineers, College Station, TX, 2015, pp. 448–461, doi: 10.1109/CPRE.2015.7102184.

[9] F. V. Lopes, M. J. B. B. Davi, M. Oleskovicz, A. Hooshyar, X. Dong, and A. A. A. Net, "Maturity Analysis of Protection Solutions for Power Systems Near Inverter-Based Resources," IEEE Transactions on Power Delivery, Vol. 39, No. 5, October 2024

[10] B. Kasztenny, M. V. Mynam, S. Marx, and R. Barone "A Novel Protection Principle for Ultra-High-Speed Tripping of Lines Terminated on Transformers," proceedings of the 16th International Conference on Developments in Power System Protection, Newcastle Gateshead, United Kingdom, March 7–10, 2022.

[11] ONS, Procedimentos de Rede—Submódulo 2.11—Requisitos mínimos para os sistemas de proteção, de registro de perturbações e de teleproteção, Revisão 2024.05. Available: www.ons.org.br.

[12] R. McDaniel, R. Chowdhury, K. Zimmerman, and B. Cockerham, "Applying SEL Relays in Systems With Inverter-Based Resources," September 2023, SEL Application Guide 2021-37. Available: www.selinc.com.

[13] E. O. Schweitzer, III, B. Kasztenny, V. Mynam, N. Fischer, and A. Guzmán, "Solving Line Protection Challenges with Transient-Based Relays," March 2023, *PAC World*. Available: www.pacw.org.

[14] H. Miller, J. Burger, N. Fischer, and B. Kasztenny, "Modern Line Current Differential Protection Solutions," 36th Annual Western Protective Relay Conference, Spokane, WA, October 2009.

[15] B. Kasztenny, "Dependability of Transient-Based Line Protection Elements and Schemes," 77th Annual Georgia Tech Protective Relaying Conference, Atlanta, GA, 2024.

[16] G. Benmouyal and J. Roberts, "Superimposed Quantities: Their True Nature and Their Application in Relays," Proceedings of the 26th Annual Western Protective Relay Conference, Spokane, WA, October 1999.

VIII. Biographies

Marcelo Bini received his BSEE in electrical engineering from Santa Catarina State University (Joinville campus), Brazil, in 2006. In 2006, he joined Engevix Engineering as an electrical engineer, working with hydroelectric power plant projects with emphasis on protection, control, and measurement systems. In 2017, he joined Araxá Solar as a substation design engineer. In 2019, he joined EDF Renewables as an electrical engineer, working with protection and control design and other electrical projects involved in substations, transmission lines, and medium-voltage networks.

Ricardo Abboud received his BS degree in electrical engineering from Uberlândia Federal University, Brazil, in 1992. In 1993, he joined CPFL Energia as a protection engineer. His responsibilities included maintenance, commissioning, specification studies, and relay settings for power system protection. In 2000, he joined Schweitzer Engineering Laboratories, Inc., (SEL), as a field application engineer in Brazil, assisting customers in substation protection and automation efforts related to generation, transmission, distribution, and industrial areas. In 2005, he became a field engineering manager, and in 2014, he became an SEL Engineering Services, Inc. (SEL ES) manager and was in charge of the SEL ES branch in Brazil. In 2016, he transferred to the SEL headquarters in Pullman, WA, as an international technical manager. In 2019, he joined SEL University as a professor, and he is currently a fellow engineer in the Sales and Customer Service division.

Fabio Lollo received his BSEE in electrical engineering from São Paulo State University (Bauru campus), Brazil, in 1997. In 1998, he joined BMG Engineering as an electrical engineer, working with protection and control design and protection studies. In 2013, he joined Schweitzer Engineering Laboratories, Inc. (SEL) as senior protection engineer in Brazil. In 2016, he became design and studies group coordinator. Currently, he is a senior protection engineer and supervises a group of project engineers with SEL Engineering Services, Inc. (SEL ES). He has experience in short-circuit calculation and protection settings for industrial and utility systems.

Paulo Lima received his BSEE in electrical engineering from Federal University of Itajubá, Brazil, in 2012. In 2013, he joined Schweitzer Engineering Laboratories, Inc. (SEL) as a protection application engineer in Brazil. In 2018, he became an application engineering group coordinator, and he has been the regional technical manager for Brazil since 2020. He has experience in application, training, integration, and testing of digital protective relays. He also provides technical writing and training associated with SEL products and SEL University.